

Assessment of Atmospheric PM₁₀ Pollution Levels and Chemical Composition in Urban Areas near the 2016 Olympic Game Arenas

Elizanne P. S. Justo,^a Maria Fernanda C. Quijano,^a Karmel Beringui,^a
Tatiana D. Saint’Pierre^a and Adriana Gioda^{✉*}

^aDepartamento de Química, Pontifícia Universidade Católica do Rio de Janeiro (PUC-Rio),
Rua Marquês de São Vicente, 225, 22451-900 Gávea-RJ, Brazil

Coarse particulate matter (PM₁₀) concentrations and chemical composition were monitored from 2014 to 2017 at three sampling sites in the Metropolitan Region of Rio de Janeiro, namely Botafogo, Gávea, and Gericinó. All sites are located close to the 2016 Olympic Game arenas. The average annual PM₁₀ concentrations were above the limits recommended by the World Health Organization (WHO) at all sampling sites. Of all the analyzed water-soluble ions, the highest concentrations were obtained for NO₃⁻, SO₄²⁻, Cl⁻ and Na⁺. Sulfate displayed a higher anthropic contribution (ca. 70%). Iron and copper were present in all samples, originated from soil resuspension and traffic (fuels and brakes, among others). Overall, civil works to restructure the city and the construction of the Olympic Game arenas increased PM₁₀ and some of its constituent levels prior to 2016. After the Olympic Games, PM₁₀ concentrations have decreased, due to governmental policies regarding traffic planning and civil work finalization.

Keywords: PM₁₀, non sea salt, secondary aerosols, 2016 Rio Olympics, chemical composition

Introduction

The atmosphere has increasingly received a high number of anthropogenic emissions, causing significant air quality alterations. Economic and demographic growth have resulted in significant gas and particle emission increases.¹ This growth, combined with the industrialization process, traffic and fuel burning, lead to high urban air pollution levels, affecting the quality of life of millions of people.²⁻⁴ Particulate matter (PM) comprises one of the essential legislated parameters for air quality assessments. Although natural sources can emit PM (such as sea salt, soil dust and plant exuding), anthropogenic sources lead to the highest contributions.⁵

High PM concentrations can induce several health problems.⁶ The World Health Organization (WHO) reports that about 4.2 million deaths *per* year are related to exposure to outdoor air pollution,⁷ and over 90% of these deaths occur as a result of non-communicable diseases, such as cardiovascular disease, stroke, chronic obstructive pulmonary disease and lung cancers.⁸⁻¹¹

The Metropolitan Region of Rio de Janeiro (MRRJ) is among the three largest megacities in South America.

This region is the second largest in terms of population concentration, industries, vehicles, and emitting pollutant sources in the country.^{12,13} The air quality in Rio de Janeiro is affected by the ocean, which favors natural ventilation, and by mountains, which hinder pollutant dispersion. Another important feature is the area’s subtropical climate, with intense solar radiation and high temperatures, which increase secondary pollutant formation.^{13,14}

In Rio de Janeiro, air pollutant monitoring for air quality assessments began in the 1960s¹² while particulate matter chemical characterization studies have been carried out since the 1980s. The first studies aimed at the chemical characterization of total suspended particles (TSP),¹⁵⁻¹⁷ followed by coarse particulate matter (PM₁₀),^{3,18,19} and, more recently, by fine particulate matter (PM_{2.5}).²⁰⁻²³

The city of Rio de Janeiro has undergone many changes, mainly concerning infrastructure and urban mobility, due to the Olympic and Paralympic Games which took place between August 5 and September 18, 2016. Works included building construction, exclusive bus routes (BRT), a new subway line (line 4), the creation of sports facilities, and roads that integrate the international airport and hotels to the Olympic arenas.²³ In addition, some measures were taken to minimize pollutant emission during the Olympic Games, such as traffic reorganization, private car

*e-mail: agioda@puc-rio.br

restrictions, street closure regarding vehicles and increased public transportation, while passenger vehicle circulation decreased.²⁴

Air quality has been a vital concern for several Olympic Game editions. For example, the Athens government worried about air quality during the 2004 Olympic Games, proposing a reduction in atmospheric pollutant (PM_{2.5}, PM₁₀, and NO_x) in order to alleviate athlete and visitor cardiopulmonary health effects during the games.^{25,26} In order to control air pollutant emissions and ensure good air quality during the Beijing 2008 Olympic Games, the Chinese government announced an "Air Quality Guarantee Plan for the 29th Olympic Games in Beijing".²⁷ Temporary measures, such as the absence of construction site work and the closure of industrial kilns during the Olympic Games led to significant pollutant reductions, and daily PM₁₀ emissions were reduced by 55%.²⁷ Black carbon, SO₂, and NO₂ were also reduced, between 30 and 50%, while PM_{2.5} was not reduced during this period.²⁸

Some studies regarding Rio de Janeiro air quality assessments have been published concerning the pre- and Olympic periods in Rio de Janeiro. One of them²⁹ refers to PM_{2.5}, PM_{2.5-10}, PM₁₀ and their chemical compositions sampled near the competition sites in Duque de Caxias, Tijuca, Taquara, and Barra da Tijuca. Another study³⁰ evaluated benzene, toluene, and xylene levels at Maracanã, Guadalupe, Jacarepaguá, Barra da Tijuca, Vila Militar, and Marina da Glória. Two other studies refer to O₃, NO₂, PM_{2.5} and PM₁₀ collected near several Olympic stations (Bangu, Campo Grande, Tijuca, Irajá, Jacarepaguá, Recreio dos Bandeirantes, Campos dos Afonsos, Gericinó, Urca, Leblon, Lagoa, Maracanã, Engenho de Dentro, and Downtown),^{31,32} while another assessed ambient air pollution (PM₁₀, SO₂, CO, O₃, NO_x) at Bangu, Irajá, São Cristovão, Tijuca, Copacabana and Centro.³³

In this context, the goals of this study were to (i) evaluate PM₁₀ levels prior (2014-2015), during (2016) and after (2017) the Olympic Games at Gávea, Gericinó and Botafogo, located near Rio 2016 arenas; (ii) determine the chemical composition of PM₁₀ obtained during 2016 and 2017, and (iii) evaluate Olympic Game impacts and the effects of the measures taken to reduce the vehicle flow on PM₁₀ levels and chemical composition.

Experimental

Sampling

PM₁₀ samples were collected at three sampling sites in the Metropolitan Region of Rio de Janeiro (MRRJ), namely Gávea, Botafogo, and Gericinó. Gávea (PUC-Rio,

22°97'88.2" S and 43°23'32.4" W), located at the PUC-Rio University, is located only a few meters from the subway line 4 works, and 200 m from an important tunnel that connects the city's south to west zones. This tunnel was used as the main link between the Copacabana and Barra da Tijuca arenas during the Olympic Games. Leblon beach and Rodrigo de Freitas Lagoon are located approximately 2 km from this station. The canoeing and rowing competitions were hosted at the lagoon during Olympic Games Rio 2016. Botafogo (BO, 22°95'31.2" S and 43°17'61.2" W) is a residential site with an intense flow of both light and heavy vehicles, mainly buses. This sampling station is located 0.5 km from the Rio de Janeiro Yacht Club, and 1.5 km from the beach volleyball stadium, in Copacabana. Gericinó (GE, 22°85'93.3" S and 43°40'80.4" W) hosted horseback riding, shooting, bicycle motocross (BMX) and grass hockey competitions during the Rio 2016 Olympic Games, and is also located near urban roads with heavy traffic (Figure 1).

The Rio de Janeiro State Environmental Institute (INEA) performed PM₁₀ sampling (GE and BO), while PUC-Rio samples were collected by our laboratory, according to Brazilian standards (ABNT-NBR 9547/86). The samples were collected using glass fiber filters (Whatman, Maidstone, United Kingdom), for 24 h every six days in a high-volume sampler (AVGPM10, Energética, São Paulo, Brazil) at an average flow rate of 1.17 m³ min⁻¹. A total of 409 PM₁₀ samples were obtained from 2014 to 2017. PM masses were determined by weighing the filters before and after sampling on an analytical balance (Mettler E., Zürich, Switzerland ± 0.0001 g). Subsequently, the filters were stored at -22 °C until analysis. At least, one sample *per* month from 2014, 2016, and 2017 was randomly selected for chemical analysis from each site, totaling 185 samples.

Chemical analyses

Sample (86.36 cm²) and blank filter (43.18 cm²) aliquots were cut and weighed using an analytical balance (Gehaka, São Paulo, Brazil, ± 0.0002 g). Twenty milliliters of ultrapure water were added to each sample, which were then shaken in a vortex mixer for 1 min and centrifuged at 2,000 rpm for 4 min. The extracts were then filtered through 0.22 μm polyethersulfone membranes (Filtrilo, Paraná, Brazil) to eliminate insoluble material. Water-soluble ions (Na⁺, NH₄⁺, K⁺, Mg²⁺, Ca²⁺, F⁻, Cl⁻, NO₂⁻, NO₃⁻, SO₄²⁻, Br⁻, PO₄³⁻) and organic acids (CH₃COO⁻, HCOO⁻, CH₂(COO)₂²⁻, (C₂O₄)²⁻) were determined using an ion chromatograph (ICS 5000, Thermo™ Scientific™ Dionex, Massachusetts, USA) equipped with a cation isocratic component, an anion gradient component and an AS-AP autosampler. Cations

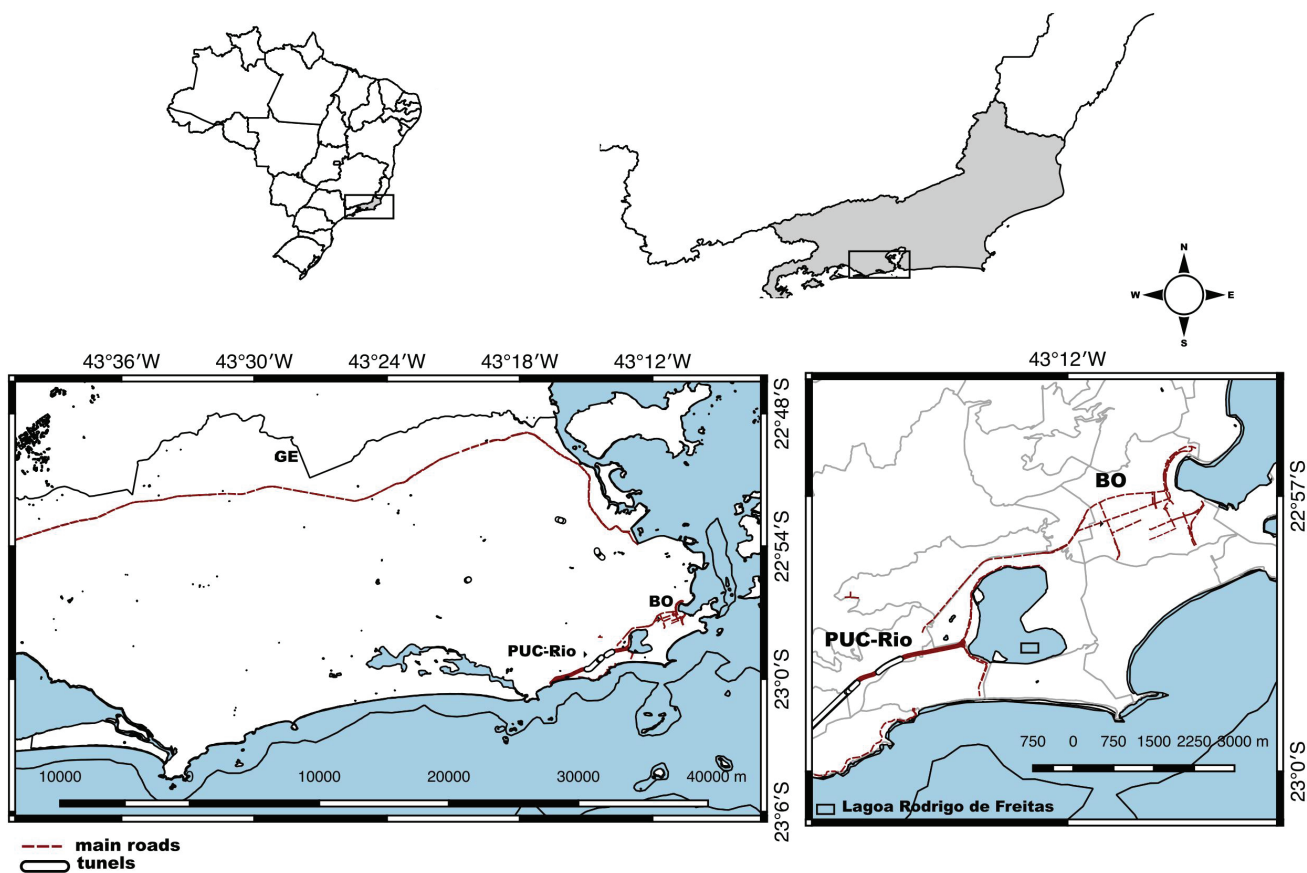


Figure 1. PM_{10} monitoring sites: BO: Botafogo, GE: Gericinó, PUC-Rio: Gávea.

were analyzed using a Dionex IonPac CS 12A column (Thermo™ Scientific™ Dionex, Massachusetts, USA) and a micro-membrane suppressor eluted with CH_3SO_2OH (18.0 mmol L^{-1}), while a Dionex IonPac AS19 column (Thermo™ Scientific™ Dionex, Massachusetts, USA) eluted with KOH (3.0 mmol L^{-1}) was used to analyze anions. The AS-AP temperature was set to $10 \text{ }^\circ\text{C}$ in order to minimize loss of volatile species. Analytical curves were prepared for both anions and cations, using standard solutions (Sigma-Aldrich, Missouri, USA) at a concentration of 1000 mg L^{-1} . The analytical curves ranged from 0.20 to 40 mg L^{-1} for anions and from 0.75 to 40 mg L^{-1} for cations. A calibration check with external standards was performed to ensure an accuracy of $\pm 10\%$.

Acid extractions were performed in order to investigate elemental compositions, applying the method previously described by Mateus and Giorda.²¹ Briefly, a strip of the sample (86.36 cm^2) and blank filters (43.18 cm^2) were cut and weighed, 5 mL of concentrated HNO_3 were added and the mixtures were then heated on a hot place at $100 \text{ }^\circ\text{C}$ for 2 h . Subsequently, the tubes were left to cool to room temperature and were then diluted to 45.0 mL with ultrapure water. Following this, the samples were centrifuged for 4 min at $2,000 \text{ rpm}$, in order to separate

any insoluble material. After the extraction, elemental compositions were determined by inductively coupled plasma mass spectrometry (ICP-MS, NexION 300X, PerkinElmer, Massachusetts, USA). A total of thirteen elements (V, Cr, Mn, Fe, Co, Ni, Cu, Cd, Pb, Ti, Mo, La, and Ce) were detected. Calibration solutions (PerkinElmer 29, PerkinElmer 17 and PerkinElmer 12, of $1000 \text{ } \mu\text{g L}^{-1}$) were prepared in ultrapure water ($5\% \text{ v/v}$) and acidified with bi-distilled HNO_3 . The analytical curve ranged from 1 to $1000 \text{ } \mu\text{g L}^{-1}$, and Rh ($40 \text{ } \mu\text{g L}^{-1}$) was used as the internal standard in an acidified aqueous solution ($5\% \text{ v/v HNO}_3$), injected on line. Operational conditions were optimized based on daily performance. All concentrations were checked against quality controls, and the coefficient of variation for this comparison was of less than 10% .

Quality assurance and quality control (QA/QC)

The efficiency of the acid extraction was evaluated by the ICP-MS analysis of the SRM1648a certified reference material (Urban dust, NIST, Maryland, USA) (Table S1, Supplementary Information (SI) section). Ultrapure water, both unfiltered and filtered, as well as HNO_3 , were also analyzed in order to verify possible contamination. Blank

filters were processed simultaneously and identically to sample filters. After removing outliers based on the Grubbs criteria, the mean blank concentrations were subtracted from the samples.

A calibration control was performed every 15 samples, in order to ensure a relative standard deviation of no more than 10%, and one sample was also analyzed in duplicate. The limit of detection (LOD) was calculated based on three times the standard deviation of the blank filters ($n = 10$) plus the mean concentrations (Table S2, SI section).

Statistical analyses

Parametric and non-parametric statistical tests were applied for PM₁₀ and chemical species concentrations for the entire study period. Differences among pollutants levels between PUC-Rio, BO and GE were determined based on analysis of variance (ANOVA) and Student's *t*-test analyses. When parametric statistical tools were inappropriate, differences were determined based on the Kruskal-Wallis analysis. Statistical significance was assessed considering a 95% confidence level ($\alpha = 0.05$). Data analyses were carried out using the R language and environment for statistical computing.³⁴

Estimation of non-sea-salt particles

In order to determine the origin of the ions detected in the samples, non-sea-salt (nss) calculations were carried, to verify sea influence, due to sampling site proximities to the coastal region. Considering Na⁺ as a reference element for sea salt, non-sea salt (nss) was calculated by the following equation:^{35,36}

$$\text{nss} - X = X_i - \text{Na}_i^+ \times (X / \text{Na}^+)_{\text{sea}} \quad (1)$$

where X_i and Na_i^+ represent the ions and Na⁺ concentrations ($\mu\text{g m}^{-3}$) in particulate matter samples, respectively, and $(X / \text{Na}^+)_{\text{sea}}$ is the ratio of each ion concentrations concerning Na⁺ in seawater. The $(X / \text{Na}^+)_{\text{sea}}$ ratios for SO₄²⁻, K⁺, Ca⁺, Cl⁻ and Mg²⁺ are 0.2516, 0.0371, 0.0385, 1.7944 and 0.1190, respectively.^{37,38}

Meteorological data

Meteorological data were obtained from INEA, through the National Institute of Meteorology (INMET) and Rio de Janeiro city Rio Alert System. Meteorological data (temperature (°C), precipitation (mm), relative humidity (%), wind direction (north, south, east, west) and wind speed (m s^{-1}) were obtained every 30 min by surface

meteorological stations located near the PM₁₀ sampling sites. The meteorological data applied to this study were 24 h means corresponding to the PM₁₀ monitored each day.

Results and Discussion

PM₁₀ concentrations

In Brazil, air quality standards are established by the Environment National Council through Resolution (RE) 03/1990,³⁹ which states that the annual arithmetic mean PM₁₀ concentration should not exceed 50 $\mu\text{g m}^{-3}$, while the mean 24-h concentration should not exceed 150 $\mu\text{g m}^{-3}$ more than once a year. A new Resolution (RE) 491/2018⁴⁰ was recently published, defining the new interim quality standards (PI), established as temporary values to be met in stages, and the final air quality standard (PF), based on guide values defined by the WHO in 2005. The new annual arithmetic mean PM₁₀ concentration is of 40 $\mu\text{g m}^{-3}$ and the daily mean concentration is of 120 $\mu\text{g m}^{-3}$, which must also not be exceeded more than once a year.⁴⁰ The present study takes into account WHO quality standards, as they were adopted by the Olympic Committee.

The annual mean PM₁₀ concentrations, standard deviation, minimum, maximum and number of daily PM exceedances according to the WHO standard are displayed in Table 1. The highest mean annual PM₁₀ concentrations were observed in 2014 at Gávea (29 $\mu\text{g m}^{-3}$) and Botafogo (34 $\mu\text{g m}^{-3}$) and in 2015 at Gericinó (44 $\mu\text{g m}^{-3}$). The highest average annual PM₁₀ concentrations were detected in 2014 and 2015, while 2016 presented the highest daily concentrations. A previous study developed in the Gávea region (2003-2005) registered an annual average of 21 $\mu\text{g m}^{-3}$,³ slightly below the values detected between 2014-2017. Gávea and Botafogo presented the lowest PM₁₀ concentrations. These regions are located near the ocean, where the sea breeze favors atmospheric pollutant dispersion.⁴¹

The annual averages observed herein exceeded the annual WHO limit (20 $\mu\text{g m}^{-3}$) during all study years. Regarding the daily values suggested by the WHO (50 $\mu\text{g m}^{-3}$), 2014 exceeded the recommended values (14%) in Botafogo and Gávea the most. The highest concentrations determined in 2014 at these sites are probably due to increased tourism, traffic and construction due to the FIFA World Cup. Gericinó registered the highest number of violations ($n = 14$) in 2015, corresponding to about 34% of the sampled days. This is probably due to the restructuring works related to urban mobility improvement and Olympic Game (2016) civil works, such as the Olympic Deodoro Park, located 0.3 km from the Gericinó station. PM₁₀ levels

were lower in 2017, exceeding the daily standard WHO ($50 \mu\text{g m}^{-3}$) by only 8%. The PM_{10} reduction observed in 2017 can be attributed to the new traffic management adopted in the city and the implementation of the Bus Rapid Transit (BRT). Improved urban mobility has resulted in an increase in daily public transport commutes, benefiting most passengers and reducing atmospheric PM emissions.⁴²

It is important to note that the daily WHO guideline was exceeded mainly during the dry period (July-September) (winter), when the 2016 Olympic Games took place. No statistically significant difference was observed when comparing the mean PM_{10} concentrations between July-September 2016 to the previous (2014-2015) and subsequent (2017) years. However, a slight decrease was observed over the years, both concerning annual means and during the dry period in all sampling locations (Table 1), which may be due to the completion of large event civil works and the implemented traffic policies.

In winter, the precipitation volume decreased by 81%, which can influence pollutant concentration increases.⁴³ The total precipitate was distributed among warmer months, during spring and summer, which comprise the seasonal wet period. In contrast, a drier period was observed in the fall

and winter months. Monthly average temperatures ranged from 19.5 to 28.3 °C. June displayed the lowest average temperature, while February was the warmest month. In addition to these variables, wind speeds ranged from 0 to 6 m s^{-1} , with weaker speeds in winter, while relative humidity reached 90% in summer. Meteorological variables may have influenced PM_{10} concentrations during the Olympic Games period, where low precipitation, low relative humidity and light winds favored increased particle concentrations.

The results obtained in Brazil during the Olympic Games are similar to other cities that have hosted this event. For example, in Athens (2004), the recorded PM_{10} values between 2001 and 2009 ranged between $30\text{--}53 \mu\text{g m}^{-3}$, depending on the sampled region. In 2004, a decrease in PM_{10} concentrations was observed, which was pronounced after 2008.²⁶ In Beijing (2008), between July-September from 2005 to 2007, previous to the Olympic Games, the average recorded PM_{10} concentration was of $123 \pm 55 \mu\text{g m}^{-3}$. However, during the Olympics, in 2008, a 33% decrease in PM_{10} levels was observed, with an average of $82 \pm 43 \mu\text{g m}^{-3}$.²⁸ The most contributing factors to high particulate matter concentrations are pollutants emitted by anthropic activities, high solar radiation levels and a high

Table 1. Descriptive statistics concentration of PM_{10} in Rio de Janeiro (2014-2017), and the number violations of the daily WHO guideline ($50 \mu\text{g m}^{-3}$)

	2014 ^a	2015	2016 ^b	2017
Gávea (PUC-Rio)				
Annual mean / ($\mu\text{g m}^{-3}$)	29.0 ± 15.7	–	25.2 ± 8.1	23.9 ± 8.6
July-September ^c mean / ($\mu\text{g m}^{-3}$)	33.3 ± 15.5	–	24.8 ± 9.1	21.3 ± 11.0
Minimum / ($\mu\text{g m}^{-3}$)	7	–	10	1
Maximum / ($\mu\text{g m}^{-3}$)	71	–	40	43
WHO violations	4	–	–	–
N	28	–	43	48
Botafogo (BO)				
Annual mean / ($\mu\text{g m}^{-3}$)	34.3 ± 12.8	33.3 ± 12.0	31.8 ± 13.9	32.2 ± 12.5
July-September ^c mean / ($\mu\text{g m}^{-3}$)	38.4 ± 15.4	35.7 ± 9.4	37.7 ± 17.7	37.7 ± 14.8
Minimum / ($\mu\text{g m}^{-3}$)	15	11	8	12
Maximum / ($\mu\text{g m}^{-3}$)	63	68	70	64
WHO violations	7	4	5	4
N	49	53	48	40
Gericinó (GE)				
Annual mean / ($\mu\text{g m}^{-3}$)	41.0 ± 18.5	44.2 ± 17.1	40.3 ± 20.5	30.5 ± 12.7
July-September ^c mean / ($\mu\text{g m}^{-3}$)	49.6 ± 20.7	53.0 ± 16.6	45.6 ± 24.6	34.4 ± 13.9
Minimum / ($\mu\text{g m}^{-3}$)	15	14	14	8
Maximum / ($\mu\text{g m}^{-3}$)	93	86	99	61
WHO violations	11	14	9	2
N	44	41	41	25

^aFIFA World Cup year; ^bOlympic Games year; ^cOlympic Games month. WHO: World Health Organization; N: sample number.

density of high buildings. However, the main reason for the increased PM₁₀ in previous Olympic Games years was the significant increase of construction works, which may have led to particle emission or resuspension.²⁵

Water-soluble ions

Table 2 presents the annual mean concentrations and standard deviations of water-soluble ions present in PM₁₀ samples. Major ions (Cl⁻, Na⁺, SO₄²⁻ and NO₃⁻) were detected at all sites, with higher concentrations in 2016 compared to 2017 (Figure 2). A significant ($p < 0.05$) decrease was observed when comparing the average major ion concentrations in July-September during the Olympic period with the same period in 2017, except for Gávea. In Gericinó and Botafogo, all ions were more concentrated in 2016, but only SO₄²⁻ was statistically different. In July-September 2017, the SO₄²⁻ concentration decreased 43 and 31% in Gericinó and Botafogo, respectively. Botafogo also presented a significantly lower annual mean NO₃⁻

concentration in 2017. At Gávea, all ions showed reduced annual mean concentrations in 2017 except for NO₃⁻, albeit non-significantly.

Cations NH₄⁺, K⁺, Mg²⁺, and Ca²⁺ were detected in all samples. The ions K⁺ and Ca²⁺ presented 46 and 30% concentrations lower at Botafogo, and 37 and 28% lower at Gericinó in 2017, respectively. Both presented a statistically significant annual concentration lower in 2017. Concerning the months corresponding to the Olympic Games, no significant difference compared to other 2016 months were observed. The NH₄⁺, K⁺, Mg²⁺, and Ca²⁺ have less anthropic contribution to their emission. The lower concentration of certain pollutants in 2017, such as Ca²⁺, is mainly due to the completion of construction works around the sampling points.

Marine contribution to particulate matter composition

Water-soluble ions are attributed to both anthropogenic and biogenic sources, such as biomass burning, fossil fuels,

Table 2. Concentrations (mean ± standard deviations) of water-soluble ions and elements in PM₁₀ in the sites: Botafogo (BO), Gávea (PUC-Rio) and Gericinó (GE)

Species	2016 PUC-Rio	2017 PUC-Rio	2016 BO	2017 BO	2016 GE	2017 GE
Na ⁺ / (µg m ⁻³)	2.74 ± 0.98	2.30 ± 0.87	3.15 ± 0.58	2.84 ± 1.11	2.76 ± 0.41	2.47 ± 0.92
K ⁺ / (µg m ⁻³)	0.27 ± 0.16	0.24 ± 0.11	0.35 ± 0.21	0.19 ± 0.08	0.46 ± 0.46	0.29 ± 0.24
Mg ²⁺ / (µg m ⁻³)	0.49 ± 0.50	0.42 ± 0.35	0.27 ± 0.08	0.25 ± 0.10	0.21 ± 0.08	0.17 ± 0.09
Ca ²⁺ / (µg m ⁻³)	0.32 ± 0.13	0.33 ± 0.12	0.56 ± 0.39	0.39 ± 0.16	0.64 ± 0.37	0.46 ± 0.26
Cl ⁻ / (µg m ⁻³)	3.86 ± 3.18	2.89 ± 1.62	3.16 ± 1.42	3.11 ± 1.62	2.50 ± 0.89	1.81 ± 0.97
NO ₃ ⁻ / (µg m ⁻³)	1.94 ± 1.02	2.15 ± 1.27	2.95 ± 1.60	1.95 ± 1.10	3.13 ± 1.09	3.01 ± 1.97
SO ₄ ²⁻ / (µg m ⁻³)	2.61 ± 1.22	2.44 ± 1.44	2.93 ± 1.18	1.69 ± 0.73	2.80 ± 1.12	1.84 ± 1.07
Org. Ac. / (µg m ⁻³)	0.42 ± 0.30	0.42 ± 0.27	0.47 ± 0.29	0.15 ± 0.09	0.49 ± 0.18	0.20 ± 0.10
NH ₄ ⁺ / (µg m ⁻³)	154 ± 170	160 ± 267	25.1 ± 25.4	28.8 ± 57.5	36.9 ± 46.3	22.6 ± 19.2
Min. An. / (µg m ⁻³)	28.1 ± 11.5	32.2 ± 16.7	19.1 ± 15.3	23.6 ± 13.7	30.4 ± 45.0	31.6 ± 14.6
V / (µg m ⁻³)	1.18 ± 0.86	1.28 ± 0.78	2.19 ± 2.01	4.36 ± 2.86	1.91 ± 1.63	2.76 ± 1.63
Cr / (ng m ⁻³)	0.94 ± 0.39	0.95 ± 0.42	3.80 ± 4.35	2.70 ± 0.98	1.88 ± 1.23	3.29 ± 1.04
Mn / (ng m ⁻³)	2.21 ± 1.18	3.73 ± 2.12	6.24 ± 7.20	8.77 ± 4.84	7.42 ± 4.83	13.3 ± 9.35
Fe / (ng m ⁻³)	124 ± 61.9	206 ± 119	312 ± 303	522 ± 289	476 ± 381	689 ± 302
Co / (ng m ⁻³)	0.03 ± 0.02	0.07 ± 0.07	0.12 ± 0.08	0.20 ± 0.05	0.17 ± 0.15	0.25 ± 0.07
Ni / (µg m ⁻³)	0.58 ± 0.38	0.46 ± 0.34	1.35 ± 0.87	1.81 ± 1.05	1.01 ± 0.65	1.48 ± 0.87
Cu / (µg m ⁻³)	15.6 ± 9.24	19.7 ± 10.8	59.0 ± 56.9	122 ± 96.1	24.3 ± 16.9	38.7 ± 40.8
Cd / (µg m ⁻³)	0.12 ± 0.07	0.16 ± 0.11	0.29 ± 0.15	0.34 ± 0.20	0.43 ± 0.36	0.63 ± 0.40
Pb / (µg m ⁻³)	1.30 ± 0.81	1.98 ± 1.60	2.70 ± 2.44	2.54 ± 1.87	5.50 ± 6.45	5.77 ± 4.45
Ti / (µg m ⁻³)	3.09 ± 2.34	3.30 ± 1.91	7.85 ± 8.42	9.78 ± 6.73	14.0 ± 14.7	15.4 ± 10.1
Mo / (µg m ⁻³)	0.29 ± 0.12	0.42 ± 0.19	0.43 ± 0.29	0.55 ± 0.29	0.34 ± 0.17	0.35 ± 0.15
La / (µg m ⁻³)	0.24 ± 0.20	0.30 ± 0.27	0.47 ± 0.30	0.61 ± 0.32	0.70 ± 0.53	1.13 ± 0.55
Ce / (µg m ⁻³)	0.33 ± 0.20	0.34 ± 0.17	0.56 ± 0.44	0.88 ± 0.57	1.09 ± 0.86	1.54 ± 0.99

ND: not detected; Org. Ac.: sum of organic acids (CH₃COO⁻, HCOO⁻, CH₂(COO)₂²⁻, (C₂O₄)²⁻); Min. An.: sum of trace anions (F⁻, NO₂⁻, Br⁻, and PO₄³⁻).

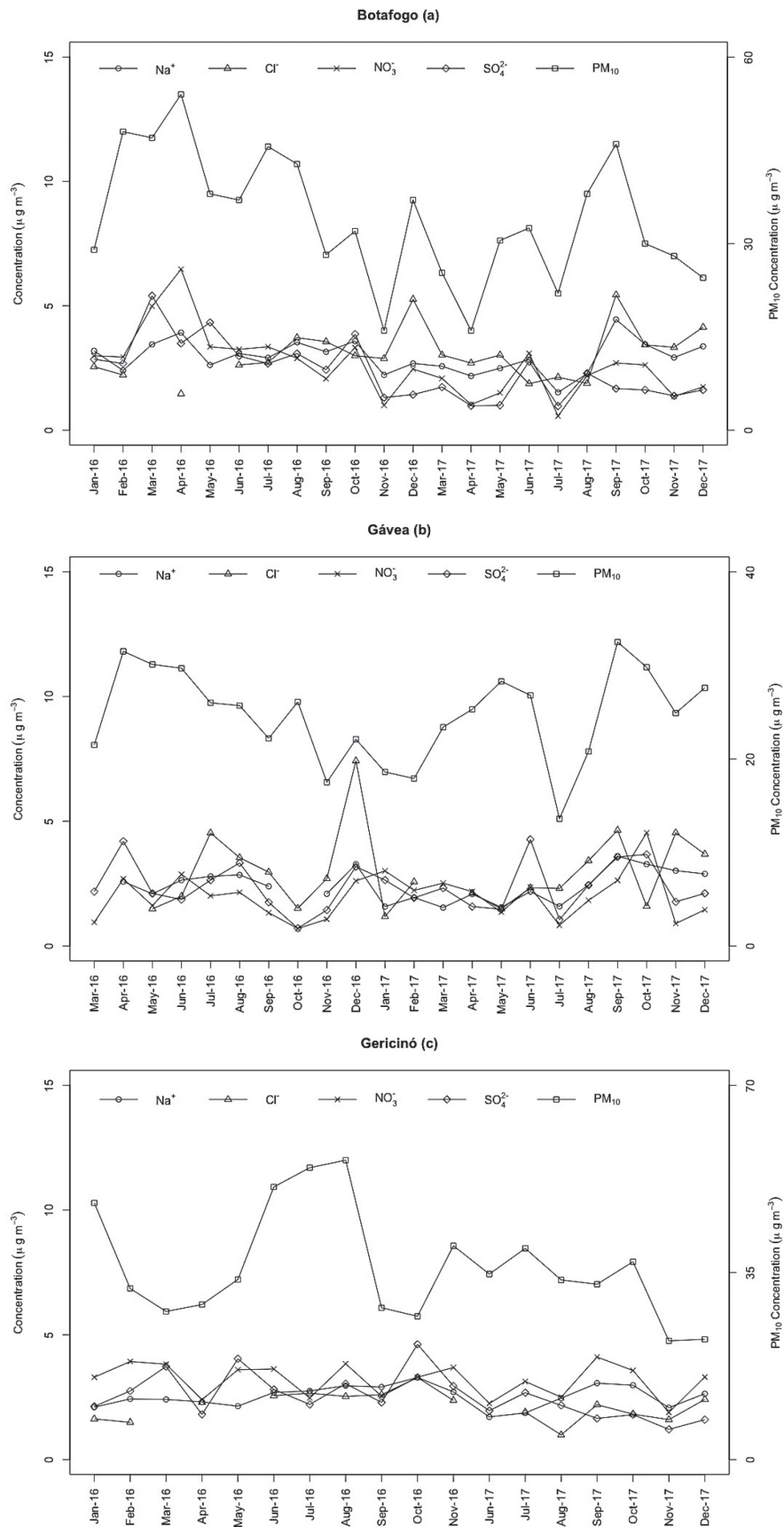


Figure 2. Temporal particulate matter and ionic species variations at (a) Botafogo, (b) Gávea and (c) Gerició.

natural plant emissions and marine aerosol particles.⁴⁴ The percentage of non-marine salt (nss) was calculated to determine the possible origin of the ions found in the samples. The sampling point locations for most of the collected samples suggest a strong sea influence, with marine spray being a possible natural source for Cl⁻, SO₄²⁻, Na⁺, K⁺, Ca²⁺ and Mg²⁺.^{38,45} Table 3 presents the ratios of ions with a non-sea salt origin.

Table 3. Inorganic non-sea-salt (nss) ion fractions in Gávea, Botafogo and Gericinó

	nss-SO ₄ ²⁻ /SO ₄ ²⁻	nss-Ca ²⁺ /Ca ²⁺	nss-K ⁺ /K ⁺
Gávea (PUC-Rio)			
2014	0.77	0.86	0.60
2016-before OG	0.76	0.75	0.52
2016-during OG	0.75	0.69	0.68
2016-after OG	0.69	0.53	0.47
2017	0.76	0.73	0.64
Botafogo (BO)			
2014	0.75	0.74	0.50
2016-before OG	0.78	0.78	0.64
2016-during OG	0.71	0.80	0.69
2016-after OG	0.71	0.71	0.59
2017	0.58	0.72	0.45
Gericinó (GE)			
2014	–	–	–
2016-before OG	0.80	0.84	0.65
2016-during OG	0.71	0.84	0.81
2016-after OG	0.80	0.78	0.72
2017	0.66	0.79	0.69

OG: Olympic Games.

The obtained results indicate no significant difference between the nss-SO₄²⁻/SO₄²⁻, nss-Ca²⁺/Ca²⁺ and nss-K⁺/K⁺ ratios for any of the studied sites. In general, the emission sources of these ions remained constant during the Olympic Games. According to the results, between 20-30% of the detected sulfate is from a marine origin, with the main source being anthropogenic (70-80%). All sites presented a similar nss-SO₄²⁻/SO₄²⁻ ratio, ranging from 0.73 to 0.77. Mateus and Gioda²¹ observed a similar contribution (75%) for nss-SO₄²⁻ in Seropédica and Santa Cruz, MRRJ sites. At Gericinó and Botafogo, nss-SO₄²⁻ emissions (58 and 66%, respectively) decreased in 2017 compared to 2016. Possible SO₄²⁻ sources include emissions from anthropogenic processes, such as fossil fuel burning, especially in urban areas, as well as a secondary process, comprising oxidation of atmospheric SO₂.^{5,46}

During the Olympic Games (winter), the marine contribution for K⁺ emissions was low, between 20-30%. In the winter, this region presented a predominance west-southwest (WSW) winds, with speeds between 0 and 6 m s⁻¹. The WSW direction has little ocean influence. After the Games, the marine contribution for K⁺ increased, of 53% in Gávea and 41% in Botafogo. In 2017 the marine percentage was of 55%, the maximum reached in Botafogo. Gericinó presented the least marine contribution, with a 28% rate after the Olympic Games. Botafogo and Gávea are located near the sea, which explains the more significant marine contribution in these sites. The nss-Ca²⁺/Ca²⁺ ratio remained constant throughout 2016 and 2017. In general, seawater Ca²⁺ emissions were low, between 15-30%. The only period with a more considerable marine contribution was Gávea in 2016 after the Olympic Games, at 47%.

In addition to seawater, Ca²⁺ and K⁺ cations are also found in soil dust and plants, representing natural sources. During transpiration, plants emit soluble K⁺ and Ca²⁺ salts, which tend to accumulate on leaf surfaces, and may therefore disperse to the atmosphere through wind. The MRRJ comprises a large part of the Atlantic Forest within the city, which may be a possible source emission of these ions. The use of civil construction cement, soil dust emissions, urban waste incineration and tire asphalt wear in large urban centers are considered anthropogenic K⁺ and Ca²⁺ emission sources.⁴⁵ The samples presenting the highest SO₄²⁻ and NO₃⁻ concentrations also contained the highest K⁺ concentrations, suggesting that fossil fuel burning is the primary source of these ions at those sites.⁴⁷

Stationary vs. mobile sources

[NO₃⁻]/[SO₄²⁻] ratios can be used as an indicator of stationary vs. mobile sulfur and nitrogen sources. Ratio values above 1 indicate the predominance of mobile sources, while values ranging from 0.1 to 0.7 suggest stationary emissions.⁴⁸ The ratios in the present study ranged from 0.30 to 1.76. At Botafogo and Gericinó, ratios were predominantly above 1, except after the 2016 Olympic Games. At Gávea, the calculated ratio suggests predominantly stationary emissions. Samplers at Botafogo, Gericinó, and Gávea are located near essential avenues with light and heavy vehicle traffic. Thus, mobile sources can be attributed mainly to combustion processes for both ions. Stationary sources can be attributed to atmospheric reactions from precursor gases, as in the case of HNO₃, which can react with soil particles such as calcium or magnesium carbonate to generate NO₃⁻.⁴⁹

Secondary species formation

Secondary species, such as ammonium sulfate ((NH₄)₂SO₄), ammonium bisulfate (NH₄HSO₄) and ammonium nitrate (NH₄NO₃), are generated by homogeneous and heterogeneous reactions of gaseous precursors, such as SO₂, NO₂ and NH₃. However, NH₄NO₃ stability decreases with increasing temperature and decreasing relative air humidity, favoring its decomposition to the gaseous forms NH₃ and HNO₃.³⁵ Squizzato *et al.*⁵⁰ reported that ammonia first neutralizes with sulfuric acid to form NH₄HSO₄ and (NH₄)₂SO₄, so the remaining ammonia would react with nitric acid to generate NH₄NO₃.

The cation NH₄⁺ was detected in all sites. The presence of this ion in PM can be due to fossil fuel burning and soil emissions.⁵¹ In the present study, NH₄⁺ emissions were predominantly associated with fossil fuels, as all sites are close to avenues presenting a high vehicular flow. Strong correlations ($r = 0.7$ to 0.8) of NH₄⁺ with nss-SO₄²⁻ throughout the sampling period were obtained. Strong correlation coefficients for NH₄⁺ and NO₃⁻ were observed only in 2016 at Gávea. A correlation of 0.80 was observed during the Olympic Game months (July-September), while a correlation of 0.90 was observed during the months following the Olympic Games (October-December). Strong correlations between NH₄⁺ and SO₄²⁻ indicate that the ammonium ion present in the atmosphere may be in the form of (NH₄)₂SO₄ or NH₄HSO₄. On the other hand, weak correlations between NH₄⁺ and NO₃⁻ for most of the samples suggest a smaller proportion in the form of NH₄NO₃. In the atmosphere, free NH₃ reacts with all H₂SO₄ present, with excess NH₃, which reacts with HNO₃, generating nitrate salts in lower amounts.^{35,45} In areas presenting NH₃ deficiency, HNO₃ cannot be neutralized from ammonia, reacting with soil characteristic coarse fraction particles to form salts.

PM₁₀ carboxylic acids

Organic anions, such as acetate, malonate, and oxalate, were also analyzed (Table 4). The highest average concentrations were observed for oxalate (155 to 566 ng m⁻³) in all sites. Oxalate has also been reported as the main carboxylic acid in other Brazilian cities (Londrina and São Paulo).^{52,53} However, in different Rio de Janeiro city regions, acetate has been reported as the predominant acid, followed by oxalate.²⁹ At Gericinó and Botafogo, a statistically significant decrease in the annual mean oxalate concentration was observed in 2017 compared to 2016. In 2016, only small changes in the mean concentrations of this compound between the months before, during and after the Olympic Games were observed. All sampling points, with

the exception of Botafogo, showed significant statistical differences when comparing average concentrations before (517 ± 291 ng m⁻³) and after (313 ± 304 ng m⁻³) the Olympic games.

In addition to oxalate, malonate (67 to 107 ng m⁻³) and acetate (35 to 73 ng m⁻³) were also detected in the PM₁₀ samples. Acetate was detected in the highest number of samples, and was observed at its highest during the Olympic Games.

In general, organic acids can be emitted into the atmosphere naturally or anthropogenically. The main natural sources are soil resuspension and vegetation. Plants contribute to about 40% of carboxylic acid emissions. In urban areas however, fuel burning is the primary source of these compounds.⁵⁴ Oxalate was strongly correlated ($r > 0.7$) to both nss-SO₄²⁻ and NO₃⁻. As SO₄²⁻ and NO₃⁻ are vehicular emission tracers, this suggests that the detected oxalate is originated from the same source. Strong correlations between nss-K⁺ oxalate were also observed ($r > 0.65$). These correlations are associated to natural (plants and soil) and anthropogenic (fossil fuel combustion) sources.

Fossil fuels burning, along with plant emissions, are also the primary sources of malonate and acetate. Possible volatilization losses were observed for these ions, as most of the samples were below the LOD.

Table 4. Average concentrations of carboxylic acid anions in PM₁₀ from Rio de Janeiro

Sampling site	Oxalate / (ng m ⁻³)	Malonate / (ng m ⁻³)	Acetate / (ng m ⁻³)
Botafogo (2014)	566 ± 380	68 ± 36	73 ± 23
Botafogo (2016)	446 ± 256	69 ± 41	38 ± 17
Botafogo (2017)	155 ± 76	ND	ND
Gávea (2014)	408 ± 344	67 ± 51	50 ± 14
Gávea (2016)	346 ± 228	88 ± 96	68 ± 38
Gávea (2017)	306 ± 171	119 ± 92	51 ± 26
Gericinó (2016)	471 ± 162	107 ± 37	35 ± 13
Gericinó (2017)	196 ± 92	ND	ND
Duque de Caxias (2012-2013) ²⁹	131 ± 62	NA	198 ± 74
Tijuca (2012-2013) ²⁹	135 ± 58	NA	220 ± 100
Taquara (2012-2013) ²⁹	122 ± 63	NA	171 ± 60
Barra da Tijuca (2012-2013) ²⁹	111 ± 55	NA	160 ± 45

ND: not detected; NA: not analyzed.

Elemental composition

Thirteen elements (V, Cr, Mn, Fe, Co, Ni, Cu, Cd, Pb, Ti, Mo, La, and Ce) were detected above the LOD. Mean

concentrations and standard deviations are presented in Table 2. Among the detected elements, Fe and Cu were the most abundant in all PM₁₀ samples. Gericinó presented the highest average Fe concentrations, with an annual means of $689 \pm 302 \text{ ng m}^{-3}$ in 2017. The year 2016 was categorized as pre, during and post-Olympic Games. In the pre-period, the mean Fe concentration was of $689 \pm 434 \text{ ng m}^{-3}$, while during and after the event values reached 326 ± 244 and $188 \pm 63 \text{ ng m}^{-3}$, respectively, with a statistically significant ($p < 0.05$) decrease among periods. In Botafogo, the mean annual Fe concentration ($522 \pm 289 \text{ ng m}^{-3}$) was higher in 2017, while in 2016 the lowest concentrations occurred during and after the Olympic Games, with no significant difference. Gávea presented the lowest Fe and Cu concentrations. In 2016, no Fe was detected during the months before the Olympic Games, while 2014 presented the highest average annual concentration, of $241 \pm 217 \text{ ng m}^{-3}$. Copper was present in the highest concentrations at Botafogo, with an annual average of $122 \pm 96 \text{ ng m}^{-3}$ in 2017. A significant decrease during the Olympic Games was observed in 2016 when compared to the months preceding the event, with a mean concentration of $43 \pm 25 \text{ ng m}^{-3}$. In 2010, high Fe and Cu concentrations were also found, with mean concentrations of $2307 \pm 42 \text{ ng m}^{-3}$ and $166 \pm 5 \text{ ng m}^{-3}$, respectively.⁵⁵ Iron can be originated from combustion sources and also from soil. Soils on roads are often enriched by elements emitted by anthropogenic sources, such as Pb, Cu, and Cd.⁵⁶ Emissions caused by brake wear also contain significant amounts of Fe, Cu and Mn.⁵⁷ The completion of the Olympic Games works may have influenced the Fe decreases observed in the post-Games period in 2016.

Among minor elements, Pb, V and Mn presented the highest concentrations. At Gericinó, these elements displayed higher average annual concentrations in 2017, while 2016 presented higher concentrations prior to the Olympic Games, with a non-significant decrease during and after the Games. Botafogo presented high Mn concentrations, especially during the Olympic Games, with an average concentration of $8 \pm 9 \text{ ng m}^{-3}$. However, no significant difference to the other assessed periods was observed. Pb and V presented average concentrations below 5 ng m^{-3} . This same pattern was observed in 2010, where $\text{Mn} > \text{V} > \text{Pb}$, with mean concentrations of 21.6 ± 0.8 , 7.8 ± 0.2 and $3.31 \pm 0.03 \text{ ng m}^{-3}$, respectively.⁵⁵

Mn and Cu also originate from the combustion processes, and are present in fossil fuels, oil, and lubricants.⁵⁸ Cu, Fe, Mn, and Pb are also present in gasoline vehicle exhaust, while Cd is present in alcohol engines and Cu is also found in additives.⁵⁷ According to Brandão *et al.*,⁵⁹ Cu, Fe, Pb and Ni are among the main metals present in Brazilian gasoline.

Correlations higher than 0.75 between V-Ni, V-Fe, and V-Mn were observed at Botafogo and Gericinó. The strong correlations between these metals indicate vehicular influence as an emission source. These sources are characteristic at these sites, due to their location close to the main city thoroughfares. Strong correlations ($r = 0.85$) were also observed between Ce and La at Botafogo and Gericinó. These metals are emitted in the atmosphere mainly from automobile gasoline.⁵⁶ Lead is also considered a tracer metal for vehicular traffic. At Gericino, Pb presented a correlation with Cd (0.86), while Cd also presented strong correlations with V. These elements represent anthropogenic pollution, mainly due to vehicular combustion. In addition to anthropogenic sources, elements from the earth's crust are also eliminated into the atmosphere, such as Ti and Mn ($r > 0.90$).

Conclusions

Long-term samplings and analyses have defined specific PM₁₀ chemical characteristics in urban Rio de Janeiro areas. The mean annual value of PM₁₀ was above the air quality limits proposed by WHO at all sites, with frequent daily violations. Differences in pollutant concentration levels at different monitoring stations were observed during the analyzed years. These differences in particulate matter levels and composition associated with the characteristic sources of each region, but also with specific and temporary sources due to the 2016 Olympic Games works. Overall, air pollution decreased during and post-Olympic Games, due to measures implemented by the local government. The 2016 Olympic Games offered rigorous measures to reduce atmospheric pollutants and lead to air quality improvements, such as road closures and truck restrictions during the Games.

This study contributes to assess air pollution impacts associated with major sporting events, and also indicates how these types of studies may work with governments to manage air pollution and how air quality can be improved for future events.

Supplementary Information

Supplementary data are available free of charge at <http://jbcs.sbq.org.br> as PDF file.

Acknowledgments

The authors thank CAPES, CNPq and FAPERJ for research grants and financial support; to LABSPECTRO for sharing their infrastructure for ICP-MS analysis; to the

technicians who assisted in the analysis: Rafael Christian Chávez Rocha and Enrique Roy Dionisio Calderon; to all the members of the Laboratory of Atmospheric Chemistry of PUC-Rio (LQA), which somehow helped during the work and INEA for providing particulate matter samples.

References

- Silveira, C.; Ferreira, J.; Monteiro, A.; Miranda, A. I.; Borrego, C.; *Air Qual., Atmos. Health* **2018**, *11*, 259.
- Amaral, B. S.; Novaes, F. J. M.; Ramos, M. C. K. V.; de Aquino Neto, F. R.; Gioda, A.; *J. Aerosol Sci.* **2016**, *100*, 155.
- Godoy, M. L. D. P.; Godoy, J. M.; Roldão, L. A.; Soluri, D. S.; Donagemma, R. A.; *Atmos. Environ.* **2009**, *43*, 2366.
- Vu, T. V.; Zauli-sajani, S.; Poluzzi, V.; Harrison, R. M.; Harrison, R. M.; *Air Qual., Atmos. Health* **2018**, *11*, 615.
- Fuzzi, S.; Baltensperger, U.; Carslaw, K.; Decesari, S.; Facchini, M. C.; Fowler, D.; Koren, I.; Langford, B.; Lohmann, U.; Nemitz, E.; Pandis, S.; Riipinen, I.; Rudich, Y.; Schaap, M.; Slowik, J. G.; Spracklen, V.; Vignati, E.; Wild, M.; Williams, M.; Gilardoni, S.; *Atmos. Chem. Phys.* **2015**, *15*, 8217.
- Kim, K.; Kabir, E.; Kabir, S.; *Environ. Int.* **2015**, *74*, 136.
- World Health Organization (WHO); *WHO Ambient Air Pollution: A Global Assessment of Exposure and Burden of Disease*, 2016. Available at <https://www.who.int/phe/publications/air-pollution-global-assessment/en/>, accessed in November 2019.
- Alves, N. O.; Brito, J.; Caumo, S.; Arana, A.; Hacon, S. S.; Artaxo, P.; Hillamo, R.; Teinila, K.; Medeiros, S. R. B.; Vasconcelos, P. C.; *Atmos. Environ.* **2015**, *120*, 277.
- Su, C.; Hampel, R.; Franck, U.; Wiedensohler, A.; Cyrus, J.; Pan, X.; Wichmann, H.-E.; Peters, A.; Schneider, A.; Breitner, S.; *Environ. Res.* **2015**, *142*, 112.
- Ribeiro, J. P.; Kalb, A. C.; Campos, P. P.; Cruz, A. R. H.; Martinez, P. E.; Gioda, A.; de Souza, M. M.; Gioda, C. R.; *Chemosphere* **2016**, *163*, 569.
- Zhang, Y.; Ji, X.; Ku, T.; Li, G.; Sang, N.; *Environ. Pollut.* **2016**, *216*, 380.
- Gioda, A.; Ventura, L. M. B.; Ramos, M. B.; Silva, M. P. R.; *Water, Air, Soil Pollut.* **2016**, *227*, 86.
- Instituto Estadual do Ambiente (INEA); *Relatório Anual da Qualidade do Ar do Estado do Rio de Janeiro*, 2009. Available at http://www.inea.rj.gov.br/cs/groups/public/@inter_dimfis_gear/documents/document/zwff/mde3/~edisp/inea_017061.pdf, accessed in November 2019.
- Instituto Estadual do Ambiente (INEA); *Relatório da Qualidade do Ar do Estado do Rio de Janeiro - Ano Base 2015*, 2016. Available at http://www.inea.rj.gov.br/cs/groups/public/@inter_dimfis_gear/documents/document/zwew/mtmx/~edisp/inea0131852.pdf, accessed in November 2019.
- Quiterio, S. L.; Silva, C. R. S.; Arbilla, G.; Escalera, V.; *Atmos. Environ.* **2004**, *38*, 321.
- Marques, L. F. C. S.; Arbilla, G.; Quiterio, S. L.; Machado, M. C. S.; *J. Braz. Chem. Soc.* **2009**, *20*, 518.
- Trindade, H. A.; Pfeiffer, W. C.; Londres, H.; Costa-Ribeiro, C. L.; *Environ. Sci. Technol.* **1981**, *15*, 84.
- Gioda, A.; Amaral, B. S.; Monteiro, I. L. G.; Saint'Pierre, T. D.; *J. Environ. Monit.* **2011**, *13*, 2134.
- Quiterio, S. L.; Arbilla, G.; Bauerfeldt, G. F.; Moreira, J. C.; *Water, Air, Soil Pollut.* **2007**, *179*, 79.
- Loyola, J.; Arbilla, G.; Quiterio, S. L.; Escalera, V.; Minho, A. S.; *J. Braz. Chem. Soc.* **2012**, *23*, 628.
- Mateus, V. L.; Gioda, A.; *Atmos. Environ.* **2017**, *164*, 147.
- Soluri, D. S.; Godoy, M. L. D. P.; Godoy, J. M.; Roldão, L. A.; *J. Braz. Chem. Soc.* **2007**, *18*, 838.
- Ventura, L. M. B.; Mateus, V. L.; Almeida, A. C. S. L.; Wanderley, K. B.; Taira, F. T.; Saint'Pierre, T. D.; Gioda, A.; *Air Qual. Atmos. Heal.* **2017**, *10*, 845.
- Companhia de Engenharia de Tráfego do RJ (CET-Rio): *Gestão do Tráfego no Jogos Olímpicos e Paralímpicos Rio 2016: Companhia de Engenharia de Tráfego*, 2016. Available at <http://www.rio.rj.gov.br/dlstatic/10112/6594316/4177742/BoletimtecnicoOlimpiadaeParalimpiada.pdf>, accessed in November 2019.
- Vassilakos, C.; Saraga, D.; Maggos, Th.; Michopoulos, J.; Pateraki, S.; Helmis, C. G.; *Sci. Total Environ.* **2005**, *349*, 223.
- Gryparis, A.; Dimakopoulou, K.; Pedeli, X.; Katsouyanni, K.; *Sci. Total Environ.* **2014**, *479-480*, 21.
- Wang, S.; Zhao, M.; Xing, J.; Wu, Y.; Zhou, Y.; Lei, Y.; He, K.; Fu, L.; Hao, J.; *Environ. Sci. Technol.* **2010**, *44*, 2490.
- Okuda, T.; Matsuura, S.; Yamaguchi, D.; Umemura, T.; Hanada, E.; Orihara, H.; Tanaka, S.; He, K.; Ma, Y.; Cheng, Y.; Liang, L.; *Atmos. Environ.* **2011**, *45*, 2789.
- Godoy, M. L. D. P.; Almeida, A. C.; Tonietto, G. B.; Godoy, J. M.; *J. Braz. Chem. Soc.* **2018**, *29*, 499.
- Araujo, B. C. C.; Lemos, M. V. P.; Oliveira, R. R. P. E.; Gil, R. A. S. S.; Siqueira, C. Y. S.; Aquino Neto, F. R.; *Microchem. J.* **2017**, *133*, 638.
- Tsuruta, F.; de Carvalho, N. J.; da Silva, C. M.; Arbilla, G.; *J. Braz. Chem. Soc.* **2018**, *29*, 1291.
- Ventura, L. M. B.; Ramos, M. B.; Santos, J. O.; Gioda, A.; *An. Acad. Bras. Cienc.* **2019**, *91*, e20170984.
- Cruz, A. R. H.; Calderon, E. R. D.; França, B. B.; Réquia, W. J.; Gioda, A.; *Atmos. Environ.* **2019**, *203*, 206.
- Team, R. C.; *R: A Language and Environment for Statistical Computing*; R Foundation for Statistical Computing, Vienna, Austria. Available at <https://www.R-project.org/>, accessed in November 2019.
- Xu, J. S.; Xu, M. X.; Snape, C.; He, J.; Behera, S. N.; Xu, H. H.; Ji, D. S.; Wang, C. J.; Yu, H.; Xiao, H.; Jiang, Y. J.; Qi, B.; Du, R. G.; *Chemosphere* **2017**, *179*, 316.
- Das, N.; Das, R.; Das, S. N.; Swamy, Y. V.; Roy Chaudhury, G.; Baral, S. S.; *Atmos. Res.* **2011**, *99*, 337.

37. McInnes, L. M.; Quinn, P. K.; Covert, D. S.; Anderson, T. L.; *Atmos. Environ.* **1996**, *30*, 869.
38. Kong, S.; Wen, B.; Chen, K.; Yin, Y.; Li, L.; Li, Q.; Yuan, L.; Li, X.; Sun, X.; *Atmos. Res.* **2014**, *147-148*, 205.
39. Conselho Nacional do Meio Ambiente (CONAMA); Resolução CONAMA No. 03, *Dispõe sobre Padrões de Qualidade do Ar; Previstos no PRONAR*; Diário Oficial da União (DOU), Brasília, de 28/06/1990, p. 15937. Available at <http://www2.mma.gov.br/port/conama/legiabre.cfm?codlegi=100>, accessed in November 2019.
40. Conselho Nacional do Meio Ambiente (CONAMA); Resolução CONAMA No. 491, *Dispõe sobre Padrões de Qualidade do Ar*; Diário Oficial da União (DOU), Brasília, No. 223, de 19/11/2018, p. 155. Available at <http://www2.mma.gov.br/port/conama/legiabre.cfm?codlegi=740>, accessed in November 2019.
41. Ventura, L. M. B.; Pinto, F. O.; Soares, L. M.; Luna, A. S.; Gioda, A.; *Meteorol. Atmos. Phys.* **2017**, *130*, 361.
42. Antonio, L.; Petzhold, G.; Bergamaschi, V.; Facchini, D.; *Res. Transp. Econ.* **2016**, *59*, 196.
43. Tang, G.; Zhang, J.; Zhu, X.; Song, T.; Münkkel, C.; Hu, B.; Schäfer, K.; Liu, Z.; Zhang, J.; Wang, L.; Xin, J.; Suppan, P.; Wang, Y.; *Atmos. Chem. Phys.* **2016**, *16*, 2459.
44. Domingos, J. S. S.; Regis, A. C. D.; Santos, J. V. S.; de Andrade, J. B.; da Rocha, G. O.; *J. Chromatogr. A* **2012**, *1266*, 17.
45. de Souza, P. A.; de Mello, W. Z.; Mariani, R. L.; Sella, S. M.; *Quim. Nova* **2010**, *33*, 1247.
46. Zhao, Y.; Gao, Y.; *Sci. Total Environ.* **2008**, *407*, 541.
47. Xiao, H.-W.; Xiao, H.-Y.; Luo, L.; Shen, C.-Y.; Long, A.-M.; Chen, L.; Long, Z.-H.; Li, D.-N.; *Atmos. Chem. Phys.* **2017**, *17*, 3199.
48. Yao, X.; Chan, C. K.; Fang, M.; Cadle, S.; Chan, T.; Mulawa, P.; He, K.; Ye, B.; *Atmos. Environ.* **2002**, *36*, 4223.
49. Anlauf, K.; Li, S. M.; Leaitch, R.; Brook, J.; Hayden, K.; Toom-Sauntry, D.; Wiebe, A.; *Atmos. Environ.* **2006**, *40*, 2662.
50. Squizzato, S.; Masiol, M.; Innocente, E.; Pecorari, E.; Rampazzo, G.; Pavoni, B.; *J. Aerosol Sci.* **2012**, *46*, 64.
51. Wang, L.; Ji, D.; Li, Y.; Gao, M.; Tian, S.; Wen, T.; Liu, Z.; Wang, L.; Xu, P.; Jiang, C.; Wang, Y.; *Atmos. Res.* **2017**, *192*, 19.
52. Vasconcellos, P. C.; Souza, D. Z.; Ávila, S. G.; Araújo, M. P.; Naoto, E.; Nascimento, K. H.; Cavalcante, F. S.; dos Santos, M.; Smichowski, P.; Behrentz, E.; *Atmos. Environ.* **2011**, *45*, 5770.
53. Freitas, A. D. M.; Martins, L. D.; Solci, M. C.; *J. Braz. Chem. Soc.* **2012**, *23*, 921.
54. da Rocha, G. O.; Vasconcellos, P. C.; Ávila, S. G.; Souza, D. Z.; Reis, E. A. O.; Oliveira, P. V.; Sanchez-Ccoyollo, O.; *J. Braz. Chem. Soc.* **2012**, *23*, 1915.
55. Silva, L. I. D.; Yokoyama, L.; Maia, L. B.; Monteiro, M. I. C.; Pontes, F. V. M.; Carneiro, M. C.; Alcover Neto, A.; *Microchem. J.* **2015**, *118*, 266.
56. Calvo, A. I.; Alves, C.; Castro, A.; Pont, V.; Vicente, A. M.; Fraile, R.; *Atmos. Res.* **2013**, *120-121*, 1.
57. Thorpe, A.; Harrison, R. M.; *Sci. Total Environ.* **2008**, *400*, 270.
58. Amaral, B. S.; Ventura, L. M. B.; Amaral, A. S.; Neto, F. R. A.; Gioda, A.; *J. Braz. Chem. Soc.* **2017**, *28*, 659.
59. Brandão, G. P.; de Campos, R. C.; de Castro, E. V. R.; de Jesus, H. C.; *Spectrochim. Acta, Part B* **2008**, *63*, 880.

Submitted: July 26, 2019

Published online: December 6, 2019

Additions and Corrections

Page 1048, Table 2, column denominated “Species”:

Where it reads:	Should be read:
NH ₄ ⁺ / (µg m ⁻³)	NH ₄ ⁺ / (ng m ⁻³)
Min. An. / (µg m ⁻³)	Min. An. / (ng m ⁻³)
V / (µg m ⁻³)	V / (ng m ⁻³)
Ni / (µg m ⁻³)	Ni / (ng m ⁻³)
Cu / (µg m ⁻³)	Cu / (ng m ⁻³)
Cd / (µg m ⁻³)	Cd / (ng m ⁻³)
Pb / (µg m ⁻³)	Pb / (ng m ⁻³)
Ti / (µg m ⁻³)	Ti / (ng m ⁻³)
Mo / (µg m ⁻³)	Mo / (ng m ⁻³)
La / (µg m ⁻³)	La / (ng m ⁻³)
Ce / (µg m ⁻³)	Ce / (ng m ⁻³)

J. Braz. Chem. Soc., Vol. 31, No. 12, 2651-2652, 2020.
<https://dx.doi.org/10.21577/0103-5053.20200198>

